Developing an Advanced Control System to Enhance Precision in Uncertain Conditions for Five-Bar Parallel Robot Through a Combination of Robust Adaptive Tracking Control Using CMAC

Tong Tan Hoa Le [1], Thanh Quyen Ngo [2*], Thanh Hai Tran [3]

[1, 2] Faculty of Electrical Engineering Technology, Industrial University of Ho Chi Minh City, Vietnam
[3] Office of Planning and Investment, Industrial University of Ho Chi Minh City, Vietnam
Email: [1] 23741961.hoa@student.iuh.edu.vn, [2] ngothanhquyen@iuh.edu.vn, [3] tranthanhhai@iuh.edu.vn
*Corresponding Author

Abstract—**Parallel robot systems have become increasingly applied due to significant advantages such as fast operating speed and high accuracy. Researchers are currently focusing on developing advanced control methods to increase the accuracy of this system. However, these advances face many challenges, including system dynamics and uncertain components in impact factors. Therefore, achieving a high level of accuracy remains a challenging problem and requires continued effort and careful research. This study proposes to use the Cerebellar Model Articulation Controller (CMAC) to estimate the nonlinear components of the system. By applying Lyapunov theory, this method focuses on adapting CMAC's online learning rules while ensuring stability and convergence. Besides using CMAC, the paper proposes a new signed distance method instead of sliding mode control (SMC) to handle input errors. This method aims to increase flexibility and adaptability and overcome the chattering of SMC in nonlinear systems. In particular, the research also adds a robust controller to ensure stability using Lyapunov to improve the system's accuracy. These recommendations increase the flexibility and accuracy of the control system, helping the system respond more quickly to changes and uncertainties in the operating environment. Finally, to demonstrate the effectiveness of the proposed controller, a five-bar parallel robot was chosen to conduct experiments in case situations. The results show that the proposed controller combined with signed distance achieves higher accuracy than other algorithms and is more stable in all cases mentioned in the research.**

Keywords—Cerebellar Model Articulation Controller; Adaptive Control; Robust Control; Signed Distance; Five-Bar Parallel Robot.

I. INTRODUCTION

In controlling complex nonlinear mechanical systems, controllers based on the mathematical model of the object often provide higher accuracy than methods not based on the mathematical model of the object. However, due to system uncertainties, such as model errors, parameter fluctuations, environmental disturbances, and initial deviations from the reference trajectory, obtaining an accurate dynamical model is complex and is not feasible. This uncertainty can reduce the accuracy of the system. In order to mitigate the impacts of uncertainty, numerous approaches have been devised, encompassing adaptive controllers [1]–[2], model predictive controllers [3]–[5], robust controllers [6]–[9], Lyapunov-based controllers [10]–[11], and sliding mode controllers (SMC) [12]–[13]. Neural networks (NNs) are built from complex parallel structures, allowing them to approximate nonlinear functions with arbitrary accuracy. Using NN to analyze the stability of uncertain dynamical systems has become popular and effective [14]–[16]. However, continuously updating all NN weights in each learning cycle is a global and time-consuming process, which limits the effectiveness of multi-layer NNs in control problems actual control [17]–[20].

The SMC structure and neural network combination have been seen as a potential approach to improve the operating accuracy of nonlinear systems [21]–[25]. However, building accurate and reliable models often poses significant challenges, leading to lower-than-expected accuracy [26]. In addressing these obstacles, numerous researchers have embraced artificial neural networks (ANN) to tackle uncertain components within mathematical models, aiming to emulate ideal sliding mode control systems [27]. These efforts address the significant challenges posed by system uncertain components and nonlinearities, which are often difficult to represent using traditional models [28]. These descriptive systems have attracted widespread interest in the literature and have many practical applications, including economics, robotics, and electrical and chemical systems [29]–[30]. However, uncertain components always exist in actual control systems, including unmodeled characteristics, model errors, and uncertain components. These conditions can reduce control system accuracy and even cause instability.

Besides the complexity of robot dynamics, one of the significant challenges for handling significant uncertain components in the dynamics [31]–[33]. The requirements for robot control systems include ensuring flexible tracking or coordination of a reference trajectory, which can vary over a specific period, along with processing uncertain situations. These are typically met through finite-time adaptive control methods [34]–[44]. Significant progress has been seen in the use of the Cerebellar Model Articulation Control (CMAC) paradigm [45]–[46] due to its fast convergence rate and good generalization ability in the identification and control of

complex dynamic systems [47]–[48]. Gradient descent algorithms such as backpropagation (BP) have been applied to optimize the parameter weights of the network model to minimize the approximation error [49]–[50]. This is a primary method for training CMAC models in system control applications. In addition, research on intelligent control has proposed methods to directly integrate human expertise into neural networks [51]–[57]. In references [48], [50], [53], and [54], some network structures were proposed combined with SMC. This is a remarkable step forward in the research and development of advanced control methods for nonlinear systems in general. However, although these controllers can adapt to actual systems, chattering emitted from the SMC can affect the system's accuracy. Chattering is a common problem in control systems, especially when using nonlinear methods such as SMC. The chattering can occur when the motion or control system is disturbed or unstable during operation. In these cases, although SMC can improve the accuracy and increase the system's flexibility, it can also introduce unwanted oscillations and increase instability in the system.

In order to minimize the chattering phenomenon from the SMC, this study designed and integrated the signed distance method into the control system. This method benefits from tracking the trajectory of nonlinear systems more accurately and stably, with gratitude for applying the Lyapunov stability theory. This article introduces the CMAC neural network model to solve the problem of estimating and adapting to nonlinear factors to improve accuracy. Besides, the research proposes a signed distance method applied to CMAC to track trajectories in nonlinear systems with uncertain components to overcome the chattering phenomenon of SMC. In addition, the stability and convergence of the CMAC adaptive law are guaranteed by the Lyapunov theory. From there, Lyapunov's theory ensures the CMAC neural network system's convergence and signed distance. Finally, the proposed structure was experimented with on a five-bar parallel robot system with many different cases to confirm the reliability of the research.

The main contributions of the research proposed in this article are summarized as follows:

1. Signed-distance method: The research introduces the method of using signed distance to overcome the chattering phenomenon generated by SMC.

2. CMAC controller: This approach combines the signed distance method with the CMAC neural network model to estimate and adapt to the nonlinear factors of the system. By using Lyapunov theory, the stability and convergence of the CMAC network structure and signed distance are guaranteed to improve the accuracy of system operation.

3. Experiment: The structure is tested on a five-bar parallel robot with many different situations to ensure the honesty and reliability of the proposed method.

The article is organized according to the following structure: Part 2 discusses the mathematical model of the five-bar parallel robot in detail. Next, in Part 3, the theory of the CMAC model is introduced. Part 4 delves into the robot's control system and describes how to analyze stability using Lyapunov. The testing process of the CMAC algorithm combined with the signed distance method is presented in Section 5. Finally, Section 6 summarizes and draws conclusions based on the information presented.

II.   DYNAMIC EQUATION DESCRIPTION

The dynamics of a five-bar parallel robot system are expressed in the Lagrange following form:

$$\boldsymbol{M}'(\boldsymbol{q}')\ddot{\boldsymbol{q}}' + \boldsymbol{C}'(\boldsymbol{q}', \dot{\boldsymbol{q}}')\dot{\boldsymbol{q}}' + \boldsymbol{g}'(\boldsymbol{q}') = \boldsymbol{\tau} \tag{1}$$

where $\boldsymbol{q}' = (q_1, q_2, q_3, q_4)^T$ represents the robot's general coordinates. $\boldsymbol{q}', \dot{\boldsymbol{q}}, \ddot{\boldsymbol{q}} \in R^{4\times1}$ are the position, velocity, and joint acceleration vectors; $\boldsymbol{M}'(\boldsymbol{q}') \in R^{4\times4}$ is the moment of inertia matrix; $\boldsymbol{C}'(\boldsymbol{q}', \dot{\boldsymbol{q}}') \in R^{4\times4}$ are the centripetal force and the Coriolis force; $\boldsymbol{g}'(\boldsymbol{q}') \in R^{4\times1}$ is the gravity vector; $\boldsymbol{\tau}$ is the control variable.
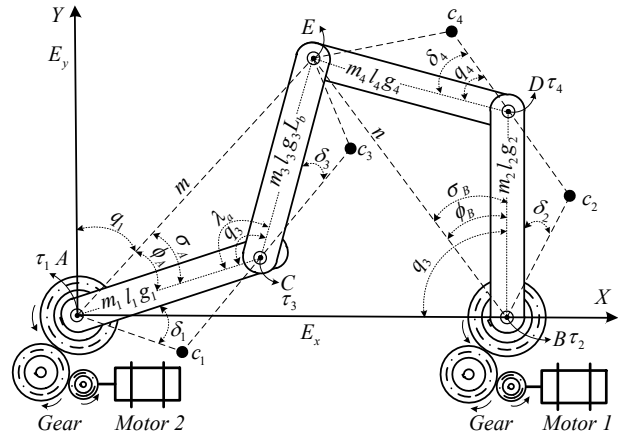

Fig. 1. Structure diagram of five-bar parallel robot

This study uses a robot model with five-bar parallel robot system as shown in Fig. 1 to evaluate the kinematic characteristics. The relationship between q_3 and q_4 is expressed based on q_1 and q_2 as follows [58]:

$$q_4 = arctan\left[\frac{\pm\sqrt{\mathcal{A}^2(q_1,q_2) + \mathcal{B}^2(q_1,q_2) - \mathcal{C}^2(q_1,q_2)}}{\mathcal{C}(q_1,q_2)}\right] \\ + arctan\left[\frac{\mathcal{B}(q_1,q_2)}{\mathcal{A}(q_1,q_2)}\right] - q_2 \tag{2}$$

$$q_3 = arctan\left[\frac{\mu(q_1,q_2) + l_4 sin(q_2 + q_4)}{\lambda(q_1,q_2) + l_4 sin(q_2 + q_4)}\right] - q_1 \tag{3}$$

$$\mathcal{A}(q_1,q_2) = 2l_4\lambda(q_1,q_2)$$

$$\mathcal{B}(q_1,q_2) = 2l_4\mu(q_1,q_2)$$

$$\mathcal{C}(q_1,q_2) = l_3^2 - l_4^2 - \lambda^2(q_1,q_2) - \mu^2(q_1,q_2)$$

$$\lambda(q_1,q_2) = l_2 cos(q_2) - l_1 cos(q_1) + l_5$$

$$\mu(q_1,q_2) = l_2 sin(q_2) - l_1 sin(q_1)$$

Moment of inertia matrix:

$$\boldsymbol{M}'(\boldsymbol{q}') = \begin{bmatrix} m_{11}' & 0 & m_{13}' & 0 \\ 0 & m_{22}' & 0 & m_{24}' \\ m_{31}' & 0 & m_{33}' & 0 \\ 0 & m_{42}' & 0 & m_{44}' \end{bmatrix} \tag{4}$$

$$m_{11}' = m_1\tau_1^2 + m_3\left(l_1^2 + \tau_3^2 + l_1\tau_3 cos(q_3 + \delta_3)\right) + J_1 + J_3$$

$$m_{13}' = m_3\left(\tau_3^2 + l_1\tau_3 cos(q_3 + \delta_3)\right) + J_3$$

$$m'_{31} = m'_{13}$$

$$m'_{22} = m_2\tau_2^2 + m_4\left(\tau_2^2 + \tau_4^2 + l_2\tau_4 cos(q_4 + \delta_4)\right) + J_2 + J_4$$

$$m'_{24} = m_4\left(\tau_3^2 + l_2\tau_4 cos(q_4 + \delta_4)\right) + J_4$$

$$m'_{42} = m'_{24}$$

$$m'_{33} = m_3\tau_3^2 + J_3$$

$$m'_{44} = m_4\tau_4^2 + J_4$$

Centripetal force is expressed as:

$$C'(q',\dot{q}') = \begin{bmatrix} \gamma_1\dot{q}_3 & 0 & \gamma_1(\dot{q}_1 + \dot{q}_3) & 0 \\ 0 & \gamma_2\dot{q}_4 & 0 & \gamma_2(\dot{q}_2 + \dot{q}_4) \\ -\gamma_1\dot{q}_1 & 0 & 0 & 0 \\ 0 & -\gamma_2\dot{q}_2 & 0 & 0 \end{bmatrix} \quad (5)$$

$$\gamma_1 = -m_3 l_1 \tau_3 sin(q_3 + \delta_3)$$

$$\gamma_2 = -m_4 l_2 \tau_4 sin(q_4 + \delta_4)$$

Gravity matrix:

$$g'(q') = 9.81 \times \begin{bmatrix} g_1 \\ g_2 \\ g_3 \\ g_4 \end{bmatrix} \quad (6)$$

$$g'_1 = (m_1\tau_1 + m_3 l_1)cos(q_1 + \delta_1) + m_3\tau_3 cos(q_1 + q_3 + \delta_3)$$

$$g'_2 = (m_2\tau_2 + m_4 l_2)cos(q_2 + \delta_2) + m_4\tau_4 cos(q_2 + q_4 + \delta_3)$$

$$g'_3 = m_3\tau_3 cos(q_1 + q_3 + \delta_3)$$

$$g'_4 = m_4\tau_4 cos(q_2 + q_4 + \delta_4)$$

However, the five-bar parallel robot system has only two control positions, represented by $q = (q_1, q_2)^T$; so there are only two control signals $\tau = (\tau_1, \tau_2)^T$. The system's dynamic model is determined in [58]–[60] as (7) to (9).

$$M(q')\ddot{q} + C(q',\dot{q}')\dot{q} + L_m\dot{q} + g(q') = \tau \quad (7)$$

$$q = \begin{bmatrix} 1 & 0 & 0 & 0 \\ 0 & 1 & 0 & 0 \end{bmatrix} q' = \rho q' \quad (8)$$

$$q' = \sigma(q) \quad (9)$$

Here, L_m is the viscosity of the motor in the system. The components of the matrix in equation (7) are calculated as follows: $M(q') = \rho^T(q')M'(q')\rho(q')$; $C(q',\dot{q}') = \rho^T(q')C'(q')\rho(q')$; $g(q') = \rho^T(q')g'(q')$.

In the nonlinear system, the state vector equation of the robot arm system is expressed:

$$\ddot{q}(t) = -\frac{C(q',\dot{q})\dot{q} + B_m\dot{q} + g(q')}{M(q')} + \frac{\tau}{M(q')} = f(\underline{x},t) + g(\underline{x},t)\tau$$

$$(10)$$

in which, $f(\underline{x},t) = -\frac{C(q',\dot{q})\dot{q} + B_m\dot{q} + g(q')}{M(q')}$ and $g(\underline{x},t) = \frac{1}{M(q')}$ are nonlinear dynamic functions that are difficult to determine. Therefore, it is impractical to design a controller based on an exact mathematical model of the object. For example, if the actual values of $f(\underline{x},t)$, $g(\underline{x},t)$ were exactly known and denoted by $F_0(\underline{x},t)$, $G_0(\underline{x},t)$ respectively. Where $F_0(\underline{x},t)$, $G_0(\underline{x},t)$ are nominal components that do not change and $L(\underline{x},t)$ is defined as the sum of the uncertain components exist in the system. The state vector $\underline{x}(t) =$

$\begin{bmatrix} x^T & \dot{x}^T & ... & x^{(n-1)T} \end{bmatrix}$ are the components of the state vector of the joint. Therefore, equation (10) is rewritten as (11):

$$\ddot{q}(t) = F_0(\underline{x},t) + G_0(\underline{x},t)\tau + L(\underline{x},t) \quad (11)$$

Control in nonlinear systems poses an important challenge. The error $e(t) \in R^{n\times1}$ must be continuously monitored and defined by subtracting the desired value $q_d(t)$ from the actual value of the system $q(t)$. The system's tracking error is described as (12):

$$e(t) = q_d(t) - q(t) \quad (12)$$

The tracking error of the system is represented in vector form as (13):

$$\underline{e}(t) = \begin{bmatrix} e^T & \dot{e}^T, ... , & e^{(n-1)T} \end{bmatrix}^T \quad (13)$$

If assume that the components $F_0(\underline{x},t)$, $G_0(\underline{x},t)$ and the sum of the uncertain components $L(\underline{x},t)$ have been determined, then the ideal controller can be designed as (14):

$$\tau_{IDEAL} = G_0^{-1}\left[\ddot{q}_d - F_0(\underline{x}) - L(\underline{x}) + K^T\underline{e}\right] \quad (14)$$

However, the problem is that it is impossible to accurately determine the parameters of the component $L(\underline{x},t)$. Therefore, the study proposes a control system described in detail in Chapter IV.

$$\tau_{controller} = \tau_{CMAC} + \tau_{RC} \quad (15)$$

The primary controller in this control structure is τ_{CMAC} to approximate the ideal controller. The aim is to maintain τ_{CMAC} as closely aligned with τ_{IDEAL} as possible. Additionally, a robust controller (τ_{RC}) is introduced to mitigate any approximation errors that arise.

The study [55] establishes that the systematic tracking error $\underline{e}$ is consolidated into signed distance $d_{si} \in R^{n\times1}$. This variable denotes the actual distance between $\underline{e}$ and the sliding surface and is shown in Fig. 2:

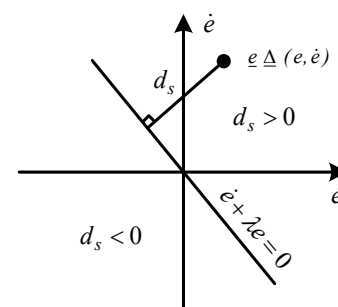$$\dot{e} + \lambda e = 0 \quad (16)$$

Fig. 2. Description of signed distance and sliding surface

where λ is the constants. The distance between the system tracking error $\underline{e}$ and the sliding surface is defined:

$$d_s = \frac{\dot{e} + \lambda e}{\sqrt{1 + \lambda^2}} = \Upsilon(\dot{e} + \lambda e) \quad (17)$$

where $\Upsilon = \frac{1}{\sqrt{1+\lambda^2}}$ is the derivative of (17). Apply the equations (12) and (15):

$$\dot{d}_s = \Upsilon(\ddot{e} + \lambda\dot{e}) = \Upsilon(-\boldsymbol{F}_0(\underline{x},t) \\ + \boldsymbol{G}_0(\underline{x},t)(\tau_{CMAC} + \tau_{RC}) \\ + \ddot{q}(t) - \boldsymbol{L}(\underline{x},t) + \lambda\dot{e}) \qquad (18)$$

The energy function of the system is defined:

$$V(d_s(t)) = \frac{1}{2}d_s^2(t) \qquad (19)$$

Multiplying equations (15) and (16):

$$d_s(t)\dot{d}_s(t) \\ = -\Upsilon(d_s(t)\boldsymbol{F}_0(\underline{x},t) \\ - d_s(t)\boldsymbol{G}_0(\underline{x},t)(\tau_{CMAC+\tau_{RC}+d_s(t)(\ddot{q}(t)-\boldsymbol{L}(\underline{x},t)+\lambda\dot{e}))} \qquad (20)$$

III. CONTROLLERS DESIGN

A. Definition of CMAC controller

Fig. 3 describes the CMAC network structure including Input space, Association memory space, Receptive-field space, Weight memory space, Output space. Details of the classes are described as follows:

1) Input space X: This is a continuous multidimensional input space. Each input state variable d_{si} is divided into separate elements and defined in a particular space for each value $X = [d_{s1}, d_{s2}]^T \in R^n$.

2) Association Memory Space, A: In this association memory space is defined as (21):

$$\mu_{ik}(d_{si}) = exp\left[\frac{-(d_{si} - m_{ik})^2}{\sigma_{ik}^2}\right] \qquad (21)$$

where m_{ik} is a translation parameter and σ_{ik} is dilation.

3) Receptive-Field Space, R: The definition of the receptive field function is showed as (22):

$$b_{jk} = \prod_{i=1}^{n_i} \mu_{ik}(d_{si}) = exp\left[\sum_{i=1}^{n_i} \frac{-(d_{si} - m_{ik})^2}{\sigma_{ik}^2}\right] \qquad (22)$$

Receptive fields can be expressed as vectors in the following manner:

$$\boldsymbol{\Delta} = [b_1 \dots b_2 \dots b_{n_k}]^T \in R^{n_k}$$

4) Weight memory space W: Each position of $\boldsymbol{\Delta}$ in this layer adjusts to a specific value denoted by:

$$\boldsymbol{W} = [w_{11} \cdots w_{1k} \cdots w_{j1} \cdots w_{jk}] \qquad (23)$$

5) Output space O: The output of CMAC is the sum of the weights, each multiplied by the superblock's corresponding activation value. The mathematical representation of the output can be described as (24):

$$\boldsymbol{O} = \sum_{j=1}^{n_j} \sum_{k=1}^{n_k} W_{jk} \prod_{i=1}^{n_i} \mu_{ik} \qquad (24)$$

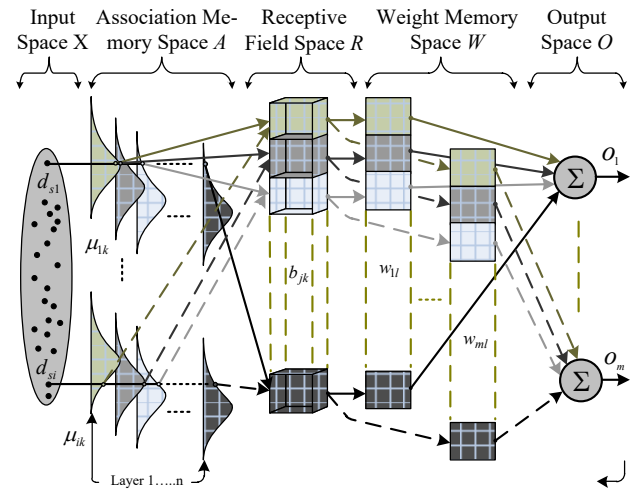For $i = 1,2,\dots,n_i,\ j = 1,2,\dots,n_j,\ k = 1,2,\dots,n_k$.

Fig. 3. Architecture of a CMAC

B. The Online Learning Rules

CMAC is described as in equation (24), in which the adaptation laws of CMAC are designed as in equations (25), (27), (28), and the robust controller is designed as in equations (26).

1) The update rule for the weight layer is derived as follows:

$$\hat{W} = -\dot{\hat{\beta}}_w \Upsilon\boldsymbol{\Delta}d_s(t) \qquad (25)$$

$$\tau_{RC} = (2R^2)^{-1}[(I + \boldsymbol{\Delta}^2)R^2 + I]d_s^T(t) \qquad (26)$$

where $R = diag[\zeta_1, \zeta_2]$ is the learning rate of the robust controller for the system to converge; $\dot{\hat{\beta}}_w$ is positive learning rate for the output weight memory w_{jk}.

2) The law for updating the parameters in the Gauss function is given as follows:

$$\dot{\hat{m}}_{ik} = \dot{\hat{\beta}}_m \Upsilon d_s(t)\hat{w}_{jk} \qquad (27)$$

$$\dot{\hat{\sigma}}_{ik} = \dot{\hat{\beta}}_\sigma \Upsilon d_s(t)\hat{w}_{jk} \qquad (28)$$

where $\dot{\hat{\beta}}_m, \dot{\hat{\beta}}_\sigma$ are positive learning rates for the translation $\hat{m}_{ik}$ and dilation $\hat{\sigma}_{ik}$.

IV. ANALYZE CONTROL STRUCTURES

Fig. 4 depicts an overview of the adaptive CMAC scheme, which includes three parts: signed distance, CMAC controller, and robust controller. An optimal parameter u_{CMAC}^* is used to estimate τ_{IDEAL} with a robust controller:

$$\tau_{IDEAL} = \tau_{CMAC}^* + \varrho = W^{*T}\mathrm{T} + \varrho \qquad (29)$$

However, in practical cases, made by estimating the nonlinear components:

$$\tau_{controller} = \tau_{CMAC} + \tau_{RC} = \hat{W}^T\boldsymbol{\Delta} + \tau_{RC} \qquad (30)$$

The Lyapunov function of this structure has the form:

$$L(s(\underline{e}), \hat{W}) = \frac{1}{2}d_s^2 + \frac{1}{2}tr[\hat{W}^T\dot{\hat{\eta}}_W^{-1}\hat{W}] \qquad (31)$$

Apply Eq. (20), (25), (26) and derivative of Eq. (31):

$$\dot{L}\big(d_s(t),\widehat{W}\big) = d_s^T(t)\dot{d}_s(t) + tr\left[\widehat{W}^T \dot{\beta}_W^{-1}\dot{\widehat{W}}\right]$$
$$= -\Upsilon(d_s(t)\boldsymbol{F}_0\big(\underline{x},t\big)$$
$$- d_s(t)\boldsymbol{G_0}\big(\underline{x},t\big)(\widehat{W}^T \boldsymbol{\Delta}$$
$$+ (2R^2)^{-1}[(I + \boldsymbol{\Delta}^2)R^2 + I]d_s{}^T(t)$$
$$+ d_s(t)(\ddot{q}(t) - \boldsymbol{L}\big(\underline{x},t\big) + \lambda\dot{e}))$$
$$+ tr\left[\widehat{W}^T\dot{\beta}_W^{-1}\dot{\widehat{W}}\right]$$
$$\leq d_s^T(t)G_0\big(\underline{x},t\big)(\widehat{W}^T\boldsymbol{\Delta}$$
$$+ (2R^2)^{-1}[(I + \boldsymbol{\Delta}^2)R^2 + I]\cdot d_s{}^T(t)$$
$$+ d_s(t)(\ddot{q}(t) - \boldsymbol{L}\big(\underline{x},t\big)$$
$$= -\frac{1}{2}d_s^T(t)\,d_s(t) \qquad (32)$$
$$- \frac{1}{2}\left[\left[\frac{d_s(t)}{\zeta} - \zeta_\varrho\right]^T\left[\frac{d_s(t)}{\zeta} - \zeta_\varrho\right]\right]$$
$$- \frac{1}{2}\left[\left[\boldsymbol{\Delta} d_s{}^T(t) - \widehat{W}\right]^T\left[\boldsymbol{\Delta} d_s{}^T(t)\right.\right.$$
$$\left.\left. - \widehat{W}\right]\right] - \widehat{W}[\Upsilon\boldsymbol{\Delta} d_s(t)]$$
$$\leq -\frac{1}{2}d_s{}^T(t)\,d_s(t) + \frac{1}{2}\zeta^2 \varrho^T \varrho$$
$$- \widehat{W}[\Upsilon\boldsymbol{\Delta} d_s(t)]$$

Integrating equation (32) from $t = 0$ to $t = T$:

$$L(T) - L(0) \;\leq\; -\frac{1}{2}\int_0^T \sum_{i=1}^n (d_{si}^2 - \zeta_i^2 \varrho_i^2 - \widehat{w}_i^2) \qquad (33)$$

Then, equation (33) is rewritten as:

$$L(T) - L(0) \;\leq\; -\frac{1}{2}\sum_{i=1}^n \int_0^T d_{si}^2(t)dt +$$
$$\frac{1}{2}\sum_{i=1}^n \zeta_i^2 \int_0^T \varrho_i^2(t)dt + \frac{1}{2}\sum_{i=1}^n \int_0^T \widehat{w}_i^2(t)dt \qquad (34)$$

The system will completely reach steady state when:

$$\frac{1}{2}\sum_{i=1}^n \int_0^T d_{si}^2(t)dt \;\leq\; L(0) +$$
$$\frac{1}{2}\sum_{i=1}^m \int_0^T \widehat{w}_k^2(t)dt + \frac{1}{2}\sum_{i=1}^n \zeta_i^2 \int_0^T \varrho_i^2(t)dt =$$
$$\frac{1}{2}d_s{}^T(0)d_s(0) + \frac{1}{2}\sum_{i=1}^n \zeta_i^2 \int_0^T \varrho_i^2(t)dt + \qquad (35)$$
$$\frac{1}{2}\sum_{i=1}^n \int_0^T \widehat{w}_i^2(t)dt$$

Adaptive CMAC Scheme Combined With Signed Distance
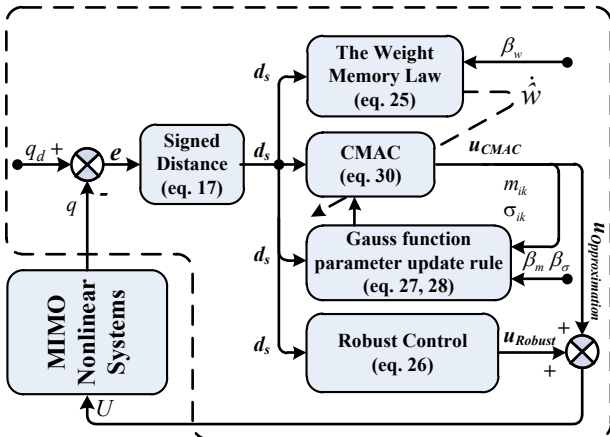

Fig. 4. Diagram depicting the CMAC control system

V.   EXPERIMENT RESULTS

In this part, the research was conducted to verify and compare the proposed method with other methods on a 5-bar parallel robot system. This decision was made based on the complexity of the system's mechanical structure while establishing an accurate mathematical model. During operation, common interactions create uncertain components that cannot be precisely determined. In addition, the viscosity and friction coefficients change during operation, causing additional control difficulties. In particular, the CMAC network is designed with signed distances to solve complex problems and can handle uncertainties in the system. The detailed mathematical model described in section II, including equations (7)-(9) and detailed parameters in Table I, plays an important role in understanding the system dynamics to allow verification of the CMAC controller. Table II talks about the network structure parameters when performing simulation experiments.

TABLE I. MODEL PARAMETERS WHEN SIMULATION

Symbol	Parameters
L_1, L_2, L_3, L_4, L_5	0.127m
m_1, m_2, m_3, m_4	0.065kg
L_m	[1,1]
$\delta_1, \delta_2, \delta_3, \delta_4$	1

TABLE II. CMAC NETWORK STRUCTURAL PARAMETERS

Symbol	Parameters
λ	200
n_k	11
$\dot{\beta}_w, \dot{\beta}_m, \dot{\beta}_\sigma$	0.25
m	(-1 1)
σ	1.2

Fig. 5 presents the robot system's structure, introducing main components such as motors, connections, and encoders. To perform experiments and collect data, we integrated the NI PCIe-6351 board with the computer and used Simulink software on the Matlab platform to control the robot arm. The control structure uses the CMAC control system combined with the signed distance method to enhance the accuracy of the five-bar parallel robot system. This combined approach was chosen to ensure operational efficiency and flexible adaptability to different conditions and environments. The study's objective is to demonstrate the superiority of using CMAC with the signed distance method compared to other control methods. Experimental results will be presented in two main parts. Part A will focus on comparing the accuracy between CMAC combined with the signed distance method and with CMAC combined with SMC and RBF in the absence of uncertainty components present to verify the contribution of the study rescue. Part B will focus on comparing the accuracy between CMAC and the signed distance method and algorithms as in part A but in the case of an uncertainty component affecting the system during operation. All algorithms will be implemented and tested on Quanser's 2-DOF robotic system, as detailed in Figure 6. This experiment will provide clear evidence of the superior accuracy of CMAC combined with the signed distance method compared to other methods based on parameters such as error and mean squared error.
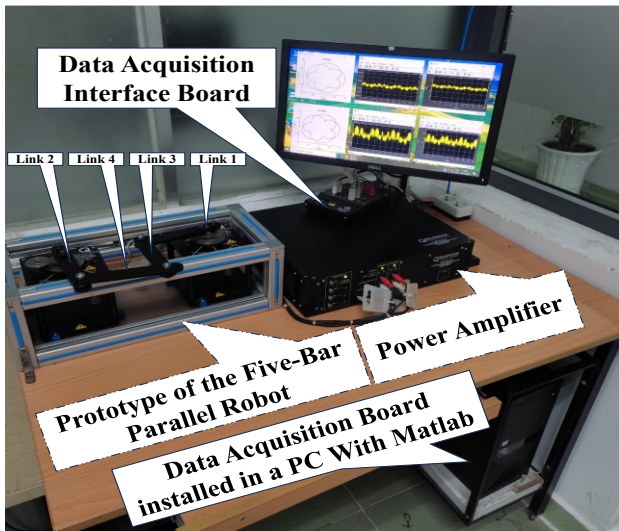
Fig. 5. Experimental system

Fig. 6. Quanser's 2 DOF Robot model

A. Experimental Results in the Absence of Uncertain Components

Fig. 7 shows the difference between the actual and reference positions of the robot joints. CMAC can maintain a stable and accurate position for both cases using signed distances and SMC. However, CMAC is combined with SMC to encounter the chattering problem of SMC. Therefore, combining CMAC with signed distance solves this problem of SMC by improved path tracking and chattering elimination. Meanwhile, the RBF algorithm can also maintain position and handling. However, its efficiency is worse than that of CMAC in both cases.

Fig. 8 describes the accuracy of the control algorithms in this study. Using CMAC in combination with signed distances to minimise errors between the actual and reference positions of the robot joints while avoiding chattering. However, as combining CMAC with SMC, the error increases due to the influence of the chattering phenomenon from SMC. However, the RBF algorithm is not better than CMAC in both combinations.

Fig. 9 shows the control voltage diagram in this experiment. It is easy to see that RBF has a wider control voltage. The accuracy is not better than that of CMAC in both cases. However, when combining CMAC with SMC, a stable voltage can be achieved like CMAC combined with the signed distance which is impossible due to the chattering.
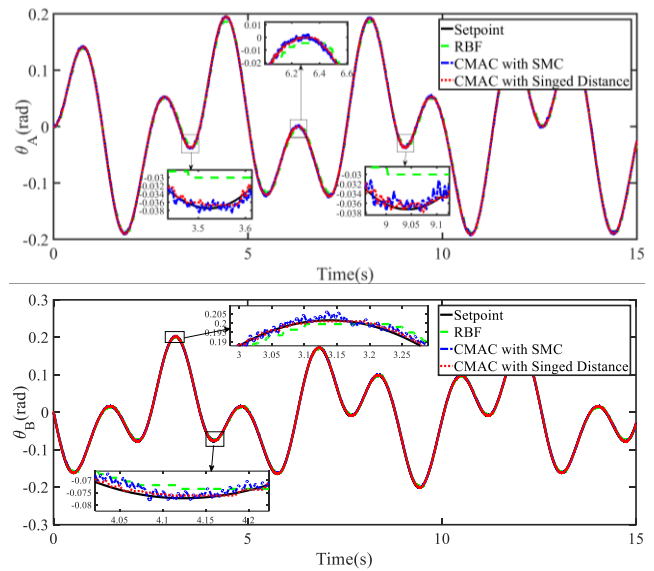

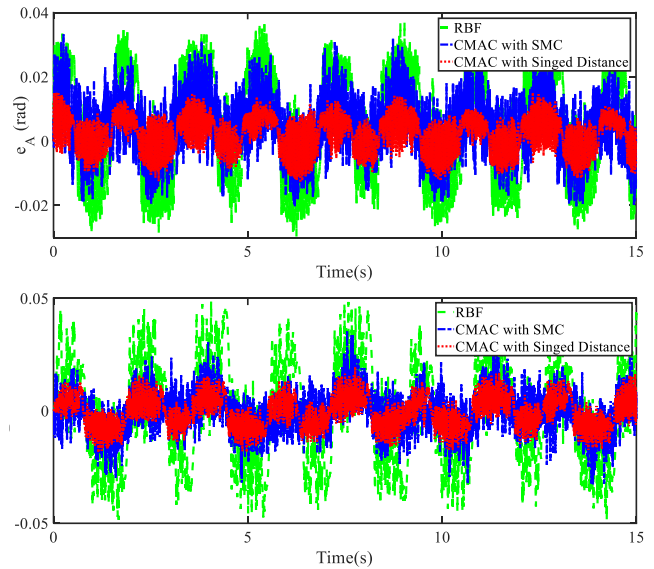Fig. 7. Actual position relative to the robot's θ_A and θ_B reference positions

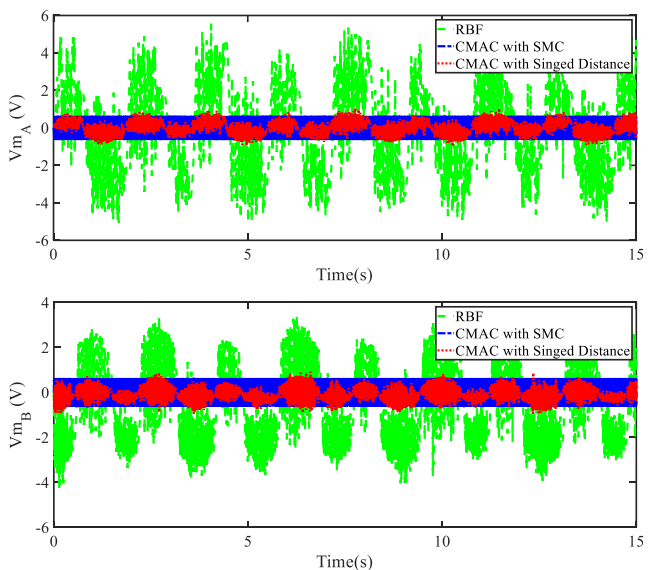Fig. 8. θ_A and θ_B error of the robot system during actual operation

Fig. 9. Control voltage of the robot system

Tong Tan Hoa Le, Developing an Advanced Control System to Enhance Precision in Uncertain Conditions for Five-Bar Parallel Robot Through a Combination of Robust Adaptive Tracking Control Using CMAC

Fig. 10 shows the difference between the actual trajectory and the reference trajectory. CMAC combined with signed distance is superior to that combined with SMC and RBF regarding tracking ability track trajectory. This demonstrates the high flexibility and adaptability of the algorithm proposed in this article.
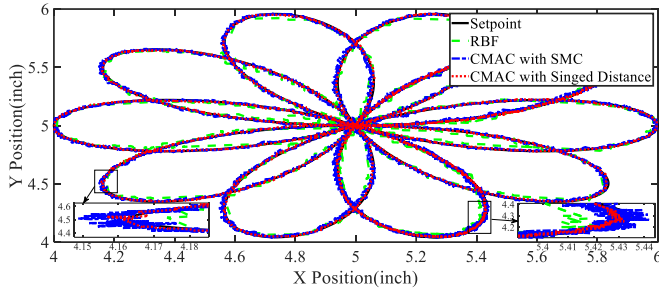

Fig. 10. Actual trajectory compared to reference trajectory when the robot system is in actual operation

In Table III, CMAC combined with signed distance shows the best accuracy with the values of e_A and mse_A are 0.825×10^{-3} and 0.682×10^{-3}, respectively. In contrast, RBF has the lowest results of e_A and mse_A are 10.75×10^{-3} and 3.044×10^{-3}, respectively. Then, CMAC with signed distance still leads to demonstrate the stability and accuracy of this method with values of e_A and mse_A are -0.534×10^{-3} and 0.382×10^{-3}, respectively. Therefore, CMAC with signed distance, which is higher accuracy than RBF, shows lower accuracy than that of but still provides an acceptable orbit tracking with corresponding e_A and mse_A values of 4.798×10^{-3} and 1.586×10^{-3} along with the corresponding e_B and mse_B values of -0.796×10^{-3} and 2.104×10^{-3}.

TABLE III. THE ACTUAL OPERATION DATA SHEET DOES NOT INCLUDE ANY UNCERTAIN COMPONENTS

Symbol	CMAC with Signed Distance ($\times 10^{-3}$)	CMAC with SMC ($\times 10^{-3}$)	RBF ($\times 10^{-3}$)
e_A	0.825	4.798	10.75
mse_A	0.682	1.586	3.044
e_B	-0.534	-0.796	0.968
mse_B	0.382	2.104	5.715

B. Experimental Results in Case of Inclusion of Uncertain Component

In order to evaluate the effectiveness of the proposed CMAC structure, it is necessary to estimate the uncertain components. The define the uncertainty components at time $t = 4$ seconds as follows: $L(\underline{x}, t) = t_l + f_l$. Where $t_l = [0.05 * \cos(t) * sign(q_1 * q_2); -0.01 * \sin(t)]$ and $f_l = [0.01 * \cos(t); -0.05 * \cos(t) * sign(q_1 * q_2)]$.

Fig. 11 shows the stability and accuracy of CMAC in maintaining the position of the robot joints. Despite uncertain components at $t = 4s$, CMAC is superior to the RBF algorithm and can still stabilize and maintain high accuracy control. Although RBF can hold position and handling, its accuracy is not as good as CMAC's, especially when including uncertain components. It is worth noting that CMAC, combined with signed distance, successfully solved the chattering problem of CMAC combined with SMC while improving accuracy and eliminating chattering during control.
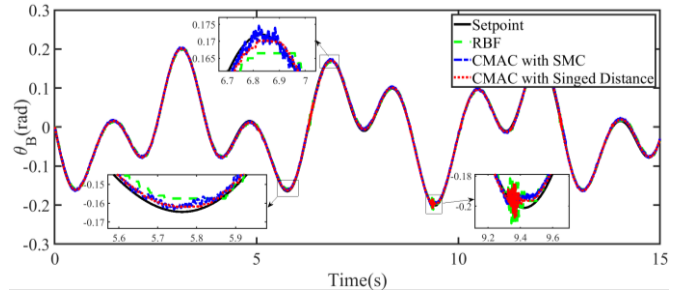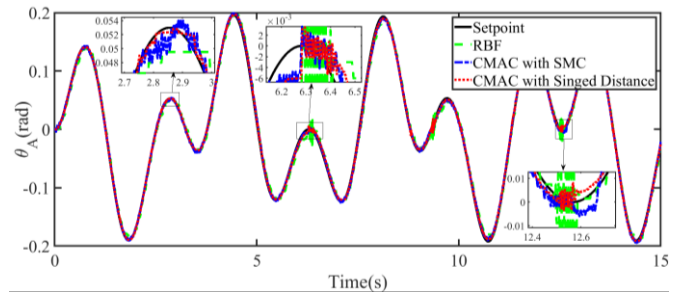

Fig. 11. Actual position relative to the robot's $\boldsymbol{\theta}_A$ and $\boldsymbol{\theta}_B$ reference positions

Fig. 12 depicts the effectiveness of CMAC in handling uncertainties in actual environments, especially at time $t = 4s$. CMAC combined with signed distance provides higher accuracy and lower error than other methods. This result is a testament to the effectiveness of the proposed method in maintaining stability and coping with fluctuations and its suitability in practical applications.
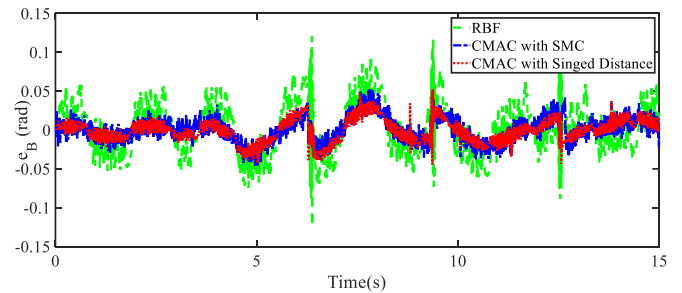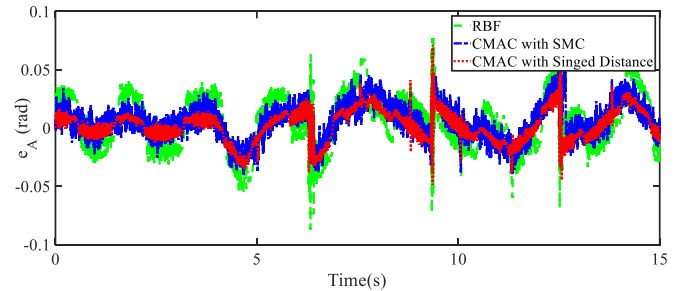

Fig. 12. $\boldsymbol{\theta}_A$ and $\boldsymbol{\theta}_B$ error of the robot system during actual operation

Fig. 13 shows the control voltage diagrams of different methods in this experiment. It is easy to see that although RBF has a more control voltage range, its accuracy is different from CMAC in both cases, especially at time $t = 4s$. When there were uncertain components, the voltage of the methods changed. However, the CMAC combined with the signed distance remained stable. Similar to the previous experiment, the voltage of CMAC combined with SMC varies significantly in a range of values of the chattering.
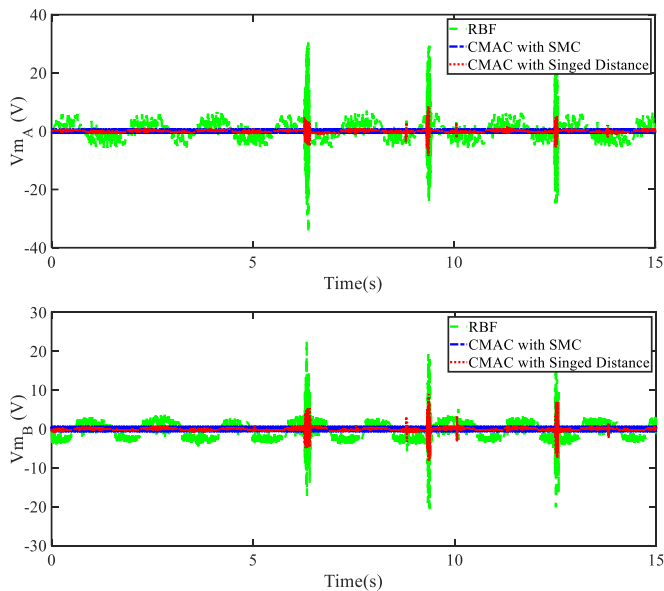
Fig. 13. The control voltage of the robot system in the case includes an uncertain component

Fig. 14 shows a comparison chart between the actual and reference trajectories. This figure shows that the combination of CMAC and signed distance outperforms the combination of CMAC combinations with SMC or RBF in trajectory tracking. This is a testament to the flexibility and high adaptability of the algorithm proposed in the study. The accuracy of different control methods can be evaluated by visually comparing the actual and reference trajectories. This result clarifies the power of CMAC combined with signed distance in achieving efficient and accurate trajectory tracking and emphasizes the algorithm's flexibility under variable environmental conditions.
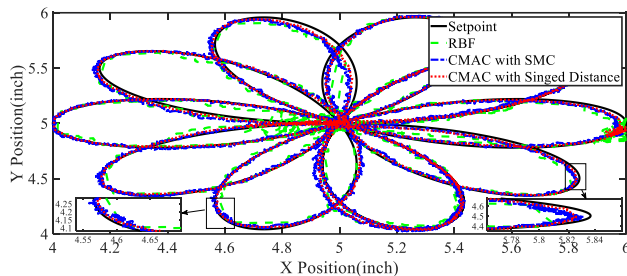

Fig. 14. Actual trajectory compared to reference trajectory when the robot system is in actual operation

Based on the data from Table IV, the CMAC method using signed distance has the best stability and accuracy in estimating the uncertain components. In comparing to CMAC using SMC and RBF, CMAC with signed distance can handle and adapt to uncertain components with according values of e_A and e_B are 0.985×10^{-3} and -0.581×10^{-3}, respectively. The results showed that the proposed structure can achieve relatively high accuracy when operating in an environment with uncertain composition. As considering mse_A and mse_B, CMAC with signed distance, which continues to hold the lowest values of 0.119×10^{-3} and 0.942×10^{-3}, respectively, compared to CMAC using SMC and RBF. This shows that CMAC with signed distance maintains higher accuracy and is more stable than the remaining methods in uncertain environments.

TABLE IV. THE ACTUAL OPERATION DATA SHEET INCLUDE UNCERTAIN COMPONENTS

Symbol	CMAC with Signed Distance ($\times10^{-3}$)	CMAC with SMC ($\times10^{-3}$)	RBF ($\times10^{-3}$)
e_A	0.985	5.30	6.60
mse_A	0.119	2.14	18.6
e_B	-0.581	0.612	0.247
mse_B	0.942	2.52	9.27e

VI. CONCLUSION AND DISCUSSION

This study is an important step forward in researching and applying new control methods in five-bar parallel robots. The choice of this experimental object is due to the mechanical complexity of the system, which makes it challenging to build an accurate mathematical model. However, this research has achieved remarkable results by combining engineering and creativity in applying a new control method based on adaptability and learning. The proposed method solves the problem of uncertain components existing in the system and enhances flexibility, stability and accuracy compared to other methods, such as RBF. Chapter 5 of the study demonstrates the feasibility and ability to overcome the chattering phenomenon of SMC. This success opens up many potential applications in important fields such as UAVs, robotics, engines, etc. This research is an important contribution to the field of five-bar parallel robotics and opens up new opportunities for applying efficient and flexible control methods in actual application.

Although this research has achieved significant progress in applying the new control method based on CMAC combined with signed distance to five-bar parallel robots, it still must be considered and overcome. One of the limitations of CMAC is that the adaptive parameters are fixed and difficult to change in complex and multivariate environments. This can reduce system accuracy when faced with fluctuations in the system. In order to overcome this, new approaches, such as integrating wavelet networks or using Brain Emotional Learning, can enhance the system's adaptive and processing capabilities. These methods can improve system accuracy and performance in more complex environments. However, it should be noted that applying new methods also requires careful consideration and control to ensure system stability and reliability. Therefore, future research can focus on developing new integration methods carefully and thoroughly testing them before implementation in actual applications.

REFERENCES

[1] J. Y. Lau, W. Liang, and K. K. Tan, "Motion control for piezoelectric-actuator-based surgical device using neural network and extended state observer," *IEEE Trans Ind. Electron.*, vol. 67, no. 1, pp. 402 -412, 2019.

[2] G. Tao, S. Chen, X. Tang, and S. M. Joshi, "Adaptive control of systems with actuator failures," *Springer Science & Business Media*, 2013.

[3] X. Zhang, J. Ma, Z. Cheng, S. Huang, S. S. Ge, and T. H. Lee, "Trajectory generation by chance-constrained nonlinear MPC with probabilistic prediction," *IEEE Trans Cybern.*, vol. 51, no. 7, pp. 3616-3629, 2020.

[4] L. Kong and J. Yuan, "Disturbance-observer-based fuzzy model predictive control for nonlinear processes with disturbances and input constraints," *ISA Trans.*, vol. 90, pp. 74–88, 2019.

[5] W. Gu, J. Yao, Z. Yao, and J. Zheng, "Output feedback model predictive control of hydraulic systems with disturbances compensation," *ISA Trans*, vol. 88, pp. 216–224, 2019.

[6] J. Ma, Z. Cheng, X. Zhang, M. Tomizuka, and T. H. Lee, "Optimal decentralized control for uncertain systems by symmetric Gauss–Seidel semi-proximal ALM," *IEEE Trans Automat. Control*, vol. 66, no. 11, pp. 5554-5560, 2021.

[7] W. Liang, S. Huang, S. Chen, and K. K. Tan, "Force estimation and failure detection based on disturbance observer for an ear surgical device," *ISA Trans*, vol. 66, pp. 476–84, 2017.

[8] J. Ma, S. -L. Chen, S. S. Teo, A. Tay, A. Al Mamun, and K. K. Tan, "Parameter space optimization towards integrated mechatronic design for uncertain systems with generalized feedback constraints," *Automatica*, vol. 105, pp. 149–58, 2019.

[9] J. Ma, Z. Cheng, H. Zhu, X. Li, M. Tomizuka, and T. H. Lee, "Convex parameterization and optimization for robust tracking of a magnetically levitated planar positioning system," *IEEE Trans Ind. Electron.*, vol. 69, no. 4, pp. 3798-3809, 2021.

[10] X. Zhang, W. Jiang, Z. Li, and S. Song, "A hierarchical Lyapunov-based cascade adaptive control scheme for lower-limb exoskeleton," *Eur. J. Control*, vol. 5, pp. 198–208, 2019.

[11] C. Shen, Y. Shi, and B. Buckham, "Trajectory tracking control of an autonomous underwater vehicle using Lyapunov-based model predictive control," *IEEE Trans Ind. Electron.*, vol. 65, .no7, pp. 5796–5805, 2017.

[12] Y. Wang, J. Chen, F. Yan, K. Zhu, and B. Chen, "Adaptive super-twisting fractional-order nonsingular terminal sliding mode control of cable-driven manipulators," *ISA Trans*, vol. 86, pp. 163–80, 2019.

[13] J. Y. Lau, W. Liang, and K. K. Tan, "Adaptive sliding mode enhanced disturbance observer-based control of surgical device," *ISA Trans*, vol. 90, pp. 178–88, 2019.

[14] C. L. P. Chen, Y.-J. Liu, and G.-X. Wen, "Fuzzy neural networkbased adaptive control for a class of uncertain nonlinear stochastic systems," *IEEE Trans. Cybern.*, vol. 44, no. 5, pp. 583–593, May 2014.

[15] C.-T. Lin, M. Prasad, and A. Saxena, "An improved polynomial neural network classifier using real-coded genetic algorithm," *IEEE Trans. Syst., Man, Cybern., Syst.*, vol. 45, no. 11, pp. 1389–1401, Nov. 2015.

[16] D. Li, C. L. P. Chen, Y. Liu, and S. Tong, "Neural network controller design for a class of nonlinear delayed systems with time-varying fullstate constraints," *IEEE Trans. Neural Netw. Learn. Syst.*, vol. 30, no. 9, pp. 2625–2636, Sep. 2019.

[17] C. Lin and C. F. Hsu, "Neural-network hybrid control for antilock braking systems," *IEEE Trans. Neural Netw.*, vol. 14, no. 2, pp. 351–359, Mar. 2003.

[18] Y. Liu, S. Liu, Y. Wang, F. Lombardi, and J. Han, "A survey of stochastic computing neural networks for machine learning applications," *IEEE Trans. Neural Netw. Learn. Syst.*, vol. 32, no. 7, pp. 2809–2824, Jul. 2021.

[19] Y.-J. Liu, L. Tang, S. Tong, and C. L. P. Chen, "Adaptive NN controller design for a class of nonlinear MIMO discrete-time systems," *IEEE Trans. Neural Netw. Learn. Syst.*, vol. 26, no. 5, pp. 1007–1018, May 2015.

[20] R. Rahimilarki, Z. Gao, A. Zhang, and R. Binns, "Robust neural network fault estimation approach for nonlinear dynamic systems with applications to wind turbine systems," *IEEE Trans. Ind. Informat.*, vol. 15, no. 12, pp. 6302–6312, Dec. 2019.

[21] W. Fang *et al*., "Visual-Guided Robotic Object Grasping Using Dual Neural Network Controllers," in *IEEE Transactions on Industrial Informatics*, vol. 17, no. 3, pp. 2282-2291, March 2021, doi: 10.1109/TII.2020.2995142.

[22] X. Guan, J. Hu, J. Qi, D. Chen, F. Zhang, and G. Yang, "Observer-based hsliding mode control for networked systems subject to communication channel fading and randomly varying nonlinearities," *Neurocomputing*, vol. 437, pp. 312–324, 2021.

[23] S. He, Y. Xu, Y. Wu, Y. Li, and W. Zhong, "Adaptive consensus tracking of multirobotic systems via using integral sliding mode control," *Neurocomputing*, vol. 455, pp. 154-162, 2021.

[24] Y. Ren, W. Zhou, Z. Li, L. Liu, and Y. Sun, "Prescribed-time leader-following consensus for stochastic second-order multi-agent systems subject to actuator failures via sliding mode control strategy," *Neurocomputing*, vol. 425, pp. 82–95, 2021.

[25] W. Wang, X. Jia, Z. Wang, X. Luo, L. Li, J. Kurths, and M. Yuan, "Fixed-time synchronization of fractional order memristive MAM neural networks by sliding mode control," *Neurocomputing*, vol. 401, pp. 364–376, 2020.

[26] W. Ji, J. Qiu, and H. R. Karimi, "Fuzzy-Model-Based Output Feedback Sliding-Mode Control for Discrete-Time Uncertain Nonlinear Systems," in *IEEE Transactions on Fuzzy Systems*, vol. 28, no. 8, pp. 1519-1530, Aug. 2020, doi: 10.1109/TFUZZ.2019.2917127.

[27] T. Q. Ngo, T. H. Tran, T. T. H. Le, and B. M. Lam, "An Application of Modified T2FHC Algorithm in Two-Link Robot Controller," *Journal of Robotics and Control (JRC)*, vol. 4, no. 4, Aug. 2023.

[28] G. Liu, S. Xu, Y. Wei, Z. Qi, and Z. Zhang, "New insight into reachable set estimation for uncertain singular time-delay systems," *Appl. Math. Comput.*, vol. 320, pp. 769–780, Mar. 2018.

[29] S. Yin, H. Gao, J. Qiu, and O. Kaynak, "Descriptor reduced-order sliding mode observers design for switched systems with sensor and actuator faults," *Automatica*, vol. 76, pp. 282–292, Feb. 2017.

[30] M. Chadli and M. Darouach, "Novel bounded real lemma for discrete-time descriptor systems: Application to H∞ control design," *Automatica*, vol. 48, no. 2, pp. 449–453, 2012.

[31] Q. Huang, Y. H. Chen, and A. Cheng, "Adaptive robust control for fuzzy mechanical systems: constraint-following and redundancy in constraints," *IEEE Trans. Fuzzy Syst*, vol. 23, no. 4, pp. 1113–1126, 2015.

[32] S. C. Zhen, X. Peng, X. L. Liu, H. M. Li, and Y. H. Chen, "A new PD based robust control method for the robot joint module," *Mech. Syst. Sig. Process*, vol. 161, 2021.

[33] X. Chen, W. Liang, H. Zhao, and A. A. Mamun, "Adaptive robust controller using intelligent uncertainty observer for mechanical systems under non-holonomic reference trajectories," *ISA Trans*, vol. 122, pp. 79–87, 2022.

[34] N. Zhou, X. Cheng, Z. Sun, and Y. Xia, "Fixed-time cooperative behavioral control for networked autonomous agents with second-order nonlinear dynamics," *IEEE Trans. Cybern*, vol. 52, no. 9, pp. 9504–9518, 2022.

[35] L. Xiao, S. Li, K. Li, L. Jin, and B. Liao, "Co-Design of Finite-Time Convergence and Noise Suppression: A Unified Neural Model for Time Varying Linear Equations With Robotic Applications," in *IEEE Transactions on Systems, Man, and Cybernetics: Systems*, vol. 50, no. 12, pp. 5233-5243, Dec. 2020, doi: 10.1109/TSMC.2018.2870489.

[36] Z. Lu, Q. Ge, Y. Li, and J. Hu, "Finite-Time Synchronization of Memristor-Based Recurrent Neural Networks With Inertial Items and Mixed Delays," in *IEEE Transactions on Systems, Man, and Cybernetics: Systems*, vol. 51, no. 5, pp. 2701-2711, May 2021, doi: 10.1109/TSMC.2019.2916073.

[37] C. -L. Hwang, F. C. Weng, W. H. Hung, F. Wu, and C. Jan, "Simultaneous translation and rotation tracking design for sharp corner, obstacle avoidance, and time-varying terrain by hierarchical adaptive fixed-time saturated control," *Mech. Syst. Sig. Process*, vol. 16, p. 107969, 2021.

[38] C. -L. Hwang and B. -S. Chen, "Adaptive Finite-Time Saturated Tracking Control for a Class of Partially Known Robots," in *IEEE Transactions on Systems, Man, and Cybernetics: Systems*, vol. 51, no. 9, pp. 5674-5685, Sept. 2021, doi: 10.1109/TSMC.2019.2957183.

[39] S. Chang, Y. Wang, Z. Zuo, and H. Yang, "Fixed-Time Formation Control for Wheeled Mobile Robots With Prescribed Performance," in *IEEE Transactions on Control Systems Technology*, vol. 30, no. 2, pp. 844-851, March 2022, doi: 10.1109/TCST.2021.3069831.

[40] D. Cruz-Ortiz, I. Chairez, and A. Poznyak, "Non-singular terminal sliding-mode control for a manipulator robot using a barrier Lyapunov function," *ISA Trans*, vol. 121, pp. 268–283, 2022.

[41] C. -L. Hwang, F. -C. Weng, D. -S. Wang, and F. Wu, "Experimental Validation of Speech Improvement-Based Stratified Adaptive Finite-Time Saturation Control of Omnidirectional Service Robot," in *IEEE Transactions on Systems, Man, and Cybernetics: Systems*, vol. 52, no. 2, pp. 1317-1330, Feb. 2022, doi: 10.1109/TSMC.2020.3018789.

[42] C. -L. Hwang and H. B. Abebe, "Generalized and Heterogeneous Nonlinear Dynamic Multiagent Systems Using Online RNN-Based Finite-Time Formation Tracking Control and Application to Transportation Systems," in *IEEE Transactions on Intelligent Transportation Systems*, vol. 23, no. 8, pp. 13708-13720, Aug. 2022, doi: 10.1109/TITS.2021.3126662.

[43] F. Sedghi, M. M. Arefi, and A. Abooee, "Command filtered-based neuro-adaptive robust finite-time trajectory tracking control of autonomous underwater vehicles under stochastic perturbations," *Neurocomputing*, vol. 519, pp. 158–172, 2023.

[44] Z. Zhu, Q. Zhu, and Q. Zhu, "Fixed-time adaptive neural self-triggered decentralized control for stochastic nonlinear systems with strong interconnections," *Neurocomputing*, vol. 523, pp. 92–102, 2023.

[45] X. Li, Z. Zhu, N. Shen, W. Dai, and Y. Hu, "Deeply feature learning by CMAC network for manipulating rehabilitation robots," *Future Generation Computer Systems*, vol. 121, pp. 19-24, 2021.

[46] N. Tan, C. Li, P. Yu, and F. Ni, "Two model-free schemes for solving kinematic tracking control of redundant manipulators using CMAC networks," *Applied Soft Computing*, vol. 126, pp. 109267, 2022.

[47] J. Albus, "A new approach to manipulator control: The cerebellar model articulation controller," *Trans. ASME J. Dyn. Syst.*, vol. 97, no. 3, pp. 270–277, 1975.

[48] W. Fang *et al.*, "A recurrent emotional CMAC neural network controller for vision-based mobile robots," *Neurocomputing*, vol. 334, pp. 227–238, Mar. 2019.

[49] H. Ying, F. Lin, and R. Sherwin, "Fuzzy discrete event systems with gradient-based online learning," in *Proc. FUZZ-IEEE Conf., New Orleans*, pp. 1–6, 2019.

[50] C. Lin, R. Ramarao, and S. Gopalai, "Self-organizing adaptive fuzzy brain emotional learning control for nonlinear systems," *Int. J. Fuzzy Syst.*, vol. 21, no. 7, pp. 1989–2007, 2019.

[51] Z. Zhong, H. -K. Lam, H. Ying and G. Xu, "CMAC-Based SMC for Uncertain Descriptor Systems Using Reachable Set Learning," in *IEEE Transactions on Systems, Man, and Cybernetics: Systems*, vol. 54, no. 2, pp. 693-703, Feb. 2024.

[52] T. Q. Ngo, M. K. Duong, D. C. Pham, and D. -N. Nguyen, "Adaptive Wavelet CMAC Tracking Control for Induction Servomotor Drive System," *Journal of Electrical Engineering & Technology*, vol. 14, no. 1, pp. 209-218, 2019.

[53] T. -T. Huynh *et al.*, "A New Self-Organizing Fuzzy Cerebellar Model Articulation Controller for Uncertain Nonlinear Systems Using Overlapped Gaussian Membership Functions," in *IEEE Transactions on Industrial Electronics*, vol. 67, no. 11, pp. 9671-9682, Nov. 2020.

[54] T. Q. Ngo, D. K. Hoang, T. T. Tran, T. T. Nguyen, V. T. Nguyen, and L. H. Le, "A Novel Self-Organizing Fuzzy Cerebellar Model Articulation Controller Based Overlapping Gaussian Membership Function for Controlling Robotic System," *International Journal Of Computers Communications & Control*, vol. 17, no. 4, p. 4606, 2022.

[55] T. Q. Ngo, T. T. H. Le, B. M. Lam, and T. K. Pham, "Adaptive Single-Input Recurrent WCMAC-Based Supervisory Control for De-icing Robot Manipulator," *Journal of Robotics and Control (JRC)*, vol. 4, no. 4, July 2023.

[56] Z. Piao, C. Guo, and S. Sun, "Adaptive Backstepping Sliding Mode Dynamic Positioning System for Pod Driven Unmanned Surface Vessel Based on Cerebellar Model Articulation Controller," in *IEEE Access*, vol. 8, pp. 48314-48324, 2020.

[57] T. Q. Ngo, T. H. Tran, and T. T. H. Le, "Robust Adaptive Tracking Control for Uncertain Five-Bar Parallel Robot Using Fuzzy CMAC in Order to Improve Accuracy," *Journal of Robotics and Control (JRC)*, vol. 5, no. 3, pp. 766-774, 2024.

[58] L. Cheng, Y. Lin, Z. -G. Hou, M. Tan, J. Huang, and W. J. Zhang, "Adaptive Tracking Control of Hybrid Machines: A Closed-Chain Five-Bar Mechanism Case," in *IEEE/ASME Transactions on Mechatronics*, vol. 16, no. 6, pp. 1155-1163, Dec. 2011.

[59] P. R. Ouyang, Q. Li, W. J. Zhang, and L. S. Guo, "Design, modeling and control of a hybrid machine system," *Mechatronics*, vol. 14, no. 10, pp. 1197–1217, 2004.

[60] F. X. Wu, W. J. Zhang, Q. Li, P. R. Ouyang, and Z. X. Zhou, "Control of hybrid machines with 2-DOF for trajectory tracking problems," *IEEE Trans. Control Syst. Technol.*, vol. 13, no. 2, pp. 338–342, Mar. 2005.